Proceedings of the 45th IEEE Conference on Decision & Control
Manchester Grand Hyatt Hotel
San Diego, CA, USA, December 13-15, 2006

6-DOF mutual synchronization of formation flying spacecraft

Thomas R. Krogstad Jan Tommy Gravdahl

Department of Engineering Cybernetics, Norwegian University of Science and Technology
Trondheim, Norway

thomas.krogstad@itk.ntnu.no tommy.gravdahl@itk.ntnu.no

Abstract— **In this paper we present a 6 degrees of freedom (6-DOF) synchronization scheme for a deep space formation of spacecraft. In the design, which is referred to as a mutual synchronization scheme, feedback interconnections are designed in such a way that the spacecraft track a time varying reference trajectory while at the same time keep a prescribed relative attitude and position. The closed-loop system is proven uniformly locally asymptotically stable, with an area of attraction which covers the complete state-space, except when the spacecraft attains an attitude where the inverse kinematics are undefined. The proof is carried out using Matrosov's Theorem.**

I. Introduction

Formation flying missions and missions involving coordinated control of several autonomous vehicles have been areas of increased interest in later years. This is due to the many inherent advantages the distributed design adds to the mission. By distributing payload on several spacecraft, redundancy is added to the system, minimizing the risk of total mission failure, several cooperating spacecraft can solve assignments which are more difficult and expensive, or even impossible with a single spacecraft, and the launch costs may be reduced since the spacecraft can be distributed on more inexpensive launch vehicles. A condition for formation flight is however a fully autonomous vehicle, as controlling spacecraft in close formation is only possible using automatic control. This results in stringent requirements on control algorithms and measurement systems.

Several control objectives can be defined depending on the specific mission of the formation. Missions may be divided into Earth observation and Space observation. Earth observation missions include missions such as Synthetic Aperture Radar (SAR) missions, where the use of a formation increases the achievable resolution of the data. In SAR missions the control objective is usually to point the payload at the same location on Earth, involving keeping the relative attitude either constant or tracking a time-varying signal depending on formation configuration and satellite orbit. Examples of planned missions are TanDEM-X [1] and SAR-Lupe [2]. Space observation missions focus on astronomical and astrophysical research outside our solar-system. The control objective usually involves keeping a constant absolute attitude in an inertial stellar system and to keep relative attitudes fixed. Examples of planned missions are XEUS [3] and DARWIN [4].

Noticeable contributions on formation control may be divided in to three separate approaches: leader-follower, behavioural and virtual structure.

In the leader-follower strategy, one spacecraft is defined as leader of the formation while the rest are defined as followers. The control objective is to enable the followers to keep a fixed relative attitude with respect to the leader [5]–[8].

The behavioural strategy views each vehicle of the formation as an agent and the control action for each agent is defined by a weighted average of the controls corresponding to the desired behaviours for the agent. This approach eases the implementation of conflicting or competing control objectives, such as tracking versus avoidance. It is however difficult to enforce group behaviour, and to mathematically guarantee stability and formation convergence. In addition, unforseen behaviour may occur when goals are conflicting. This strategy is widely reported for use on mobile robots [9]–[11], and was also applied to spacecraft formations in [12].

In the virtual structure approach, the formation is defined as a virtual rigid body. In this approach the problem is how to define the desired attitude and position for each member of the formation such that the formation as a whole moves as a rigid body. In this scheme it is easy to prescribe a coordinated group behaviour and to maintain the formation during maneuvers. But the actual performance is however dependent on the individual member's control system's ability to track the desired trajectories. Virtual structures were applied to mobile robots in [13] and more recently to spacecraft formations in [14], [15].

In this work we apply theory derived in [8], on mutual synchronization of robot manipulators, to design a synchronization scheme for a formation of autonomous spacecraft. The formation is assumed to be located such that influences from celestial objects can be ignored, a location often referred to as *deep space* in the literature. The goal is to have the attitude and position of each spacecraft track a desired trajectory, while simultaneously making sure that the spacecraft is synchronized with respect to the other formation members. The approach may be viewed as a combination of the leader-follower approach with a virtual leader and the behavioural approach, in that the spacecraft must attempt to achieve two possibly conflicting goals.

The paper is organized as follows: Section II gives a general introduction to modelling and equations of motion, in Section III we propose and prove our main idea, then we include a simulation of a 3 satellite formation in Section IV and conclusions are made in V.

II. MODELLING

In this section we derive equations of motion for a spacecraft actuated by means of reaction wheels and thrusters, using the notation of [16], [17] and [18].

A. Reference frames

Equations of motion will be expressed in two different reference frames. A general reference frame will be denoted as $\mathcal{F}$ with a subscript corresponding to a given frame.

1) Inertial frame: This frame is an inertial frame for the spacecraft motion. Since the formation is in deep space, an example is a sun centered frame which is inertial for motion in the solar system or a star centered frame which is inertial in celestial space. We denote this frame $\mathcal{F}_i$.

2) Body-fixed reference frame: This reference frame has its origin in the center of gravity of the spacecraft, with axes pointing along the principal axes of inertia of the spacecraft. The frame is denoted $\mathcal{F}_b$ for a general body frame and $\mathcal{F}_{bk}$ for $k \in \{1, \ldots, n\}$, where n is the number of spacecraft in the formation.

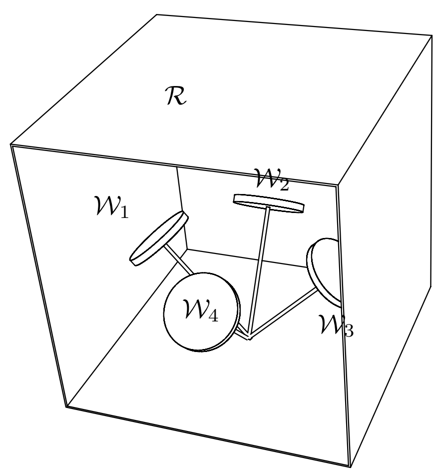

Fig. 1. Illustration of a gyrostat with four reaction wheels in a tetrahedron configuration.

B. Kinematics

The attitude kinematics is described in Euler angles, using the roll-pitch-yaw notation. In this notation a three element vector $\mathbf{\Theta} = [\theta, \phi, \psi]^T$ is used to describe the attitude of the spacecraft with respect to a reference frame, with corresponding rotation matrix

$$\mathbf{R}_b^a(\mathbf{\Theta}) = \mathbf{R}_z(\psi)\mathbf{R}_y(\theta)\mathbf{R}_x(\phi), \tag{1}$$

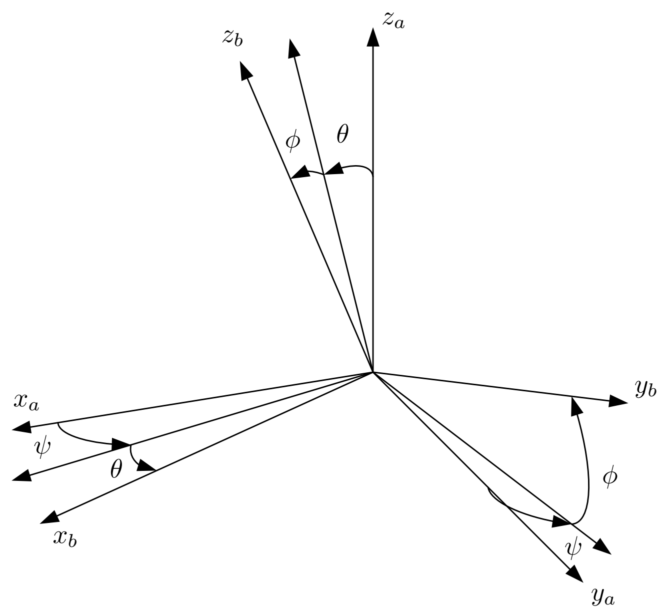

Fig. 2. The figure illustrates how rotation between two frames can be interpreted in form of Euler angles.

where $\mathbf{R}_z(\psi)$, $\mathbf{R}_y(\theta)$ and $\mathbf{R}_x(\phi)$ are simple rotations, given by

$$\mathbf{R}_x(\phi) = \begin{bmatrix} 1 & 0 & 0 \\ 0 & \cos\phi & -\sin\phi \\ 0 & \sin\phi & \cos\phi \end{bmatrix} \tag{2}$$

$$\mathbf{R}_y(\theta) = \begin{bmatrix} \cos\theta & 0 & \sin\theta \\ 0 & 1 & 0 \\ -\sin\theta & 0 & \cos\theta \end{bmatrix} \tag{3}$$

$$\mathbf{R}_z(\psi) = \begin{bmatrix} \cos\psi & -\sin\psi & 0 \\ \sin\psi & \cos\psi & 0 \\ 0 & 0 & 1 \end{bmatrix}. \tag{4}$$

Such a rotation may be illustrated as in Fig. 4.

A kinematic differential equation is derived by noting that

$$\boldsymbol{\omega} = \begin{bmatrix} \dot\phi \\ 0 \\ 0 \end{bmatrix} + \mathbf{R}_x(\phi)\begin{bmatrix} 0 \\ \dot\theta \\ 0 \end{bmatrix} + \mathbf{R}_x(\phi)\mathbf{R}_y(\theta)\begin{bmatrix} 0 \\ 0 \\ \dot\psi \end{bmatrix} \tag{5}$$

$$= \begin{bmatrix} 1 & 0 & -\sin\theta \\ 0 & \cos\phi & \sin\phi\cos\theta \\ 0 & -\sin\phi & \cos\phi\cos\theta \end{bmatrix}\dot{\mathbf{\Theta}} = \mathbf{T}(\mathbf{\Theta})^{-1}\dot{\mathbf{\Theta}}, \tag{6}$$

and thereby obtaining the kinematic differential equation

$$\dot{\mathbf{\Theta}} = \mathbf{T}(\mathbf{\Theta})\boldsymbol{\omega}, \tag{7}$$

where

$$\mathbf{T}(\mathbf{\Theta}) = \frac{1}{\cos\theta}\begin{bmatrix} \cos\theta & \sin\phi\sin\theta & \cos\phi\sin\theta \\ 0 & \cos\phi\cos\theta & \sin\phi\cos\theta \\ 0 & \sin\phi & \cos\phi \end{bmatrix}. \tag{8}$$

C. Dynamics

1) Attitude dynamics: The attitude dynamics relates the change of angular momentum to the applied control and disturbance moments. We derive the differential equations governing this relation using vectorial mechanics and the Newton-Euler formulation for a spacecraft actuated by means of redundant reaction wheels, a system commonly referred to as a *gyrostat* [17], as illustrated in Fig. 1.

We start by writing the total angular momentum of the gyrostat in $\mathcal{F}_b$ and the total axial angular momentum of the wheels

$$\mathbf{h}^b = \mathbf{J}\boldsymbol{\omega}_{ib}^b + \mathbf{A}\mathbf{I}_s\boldsymbol{\omega}_s \tag{9a}$$
$$\mathbf{h}_a = \mathbf{I}_s\mathbf{A}^T\boldsymbol{\omega}_{ib}^b + \mathbf{I}_s\boldsymbol{\omega}_s, \tag{9b}$$

where $\mathbf{A} \in \mathbb{R}^{3\times 4}$ is a matrix of wheel axes in $\mathcal{F}_b$ given by (10), $\mathbf{I}_s \in \mathbb{R}^{4\times 4}$ a diagonal matrix of wheel axial inertias, $\boldsymbol{\omega}_s \in \mathbb{R}^4$ a vector of wheel velocities and $\mathbf{J} \in \mathbb{R}^{3\times 3}$ the total moment of inertia. $\mathbf{A}$ is dependent on the geometric placement of the wheels. In [19], four wheels in tetrahedron configuration were employed. In that case the matrix is given by

$$\mathbf{A} = \begin{bmatrix} \sqrt{\frac{1}{3}} & \sqrt{\frac{1}{3}} & -\sqrt{\frac{1}{3}} & -\sqrt{\frac{1}{3}} \\ \sqrt{\frac{2}{3}} & -\sqrt{\frac{2}{3}} & 0 & 0 \\ 0 & 0 & -\sqrt{\frac{2}{3}} & \sqrt{\frac{2}{3}} \end{bmatrix}, \tag{10}$$

which will also be used here.

Assuming that the body frame coincides with the center of gravity, we may express the change of angular momentum as

$$\dot{\mathbf{h}}^b = (\mathbf{h}^b)^\times \bar{\mathbf{J}}^{-1}(\mathbf{h}^b - \mathbf{A}\mathbf{h}_a) + \boldsymbol{\tau}_d^b \tag{11a}$$
$$\dot{\mathbf{h}}_a = \boldsymbol{\tau}_a, \tag{11b}$$

where $(\cdot)^\times$ is the skew-symmetric operator, mapping from $\mathbb{R}^3$ to $\mathbb{R}^{3\times 3}$ according to

$$(\mathbf{z})^\times \triangleq \begin{bmatrix} 0 & -z_3 & z_2 \\ z_3 & 0 & -z_1 \\ -z_2 & z_1 & 0 \end{bmatrix}, \tag{12}$$

$\bar{\mathbf{J}} \in \mathbb{R}^{3\times 3}$ is an inertia-like matrix defined as

$$\bar{\mathbf{J}} \triangleq \mathbf{J} - \mathbf{A}\mathbf{I}_s\mathbf{A}^T$$

and $\boldsymbol{\tau}_d^b$ is the resultant external torques due to position control and environmental disturbances.

Remark 1: When controlling attitude using reaction wheels angular momentum will build up due to non-cyclic disturbance torques. This leads to a steady increase of wheel speeds, until a saturation level is reached and no more control can be achieved. The reaction wheels must then be desaturated by applying a external torque, see [20] for an example of how this can be done.

Equation (11) may also be expressed in terms of angular velocities as

$$\mathbf{J}\dot{\boldsymbol{\omega}}_{ib}^b = (\mathbf{J}_b\boldsymbol{\omega}_{ib}^b)^\times\boldsymbol{\omega}_{ib}^b + (\mathbf{A}\mathbf{I}_s\boldsymbol{\omega}_s)^\times\boldsymbol{\omega}_{ib}^b - \mathbf{A}\boldsymbol{\tau}_a + \boldsymbol{\tau}_d \tag{13a}$$
$$\mathbf{I}_s\dot{\boldsymbol{\omega}}_s = \boldsymbol{\tau}_a - \mathbf{I}_s\mathbf{A}\dot{\boldsymbol{\omega}}_{ib}^b \tag{13b}$$

For the purpose of control design we rewrite the model in terms of Euler angles and their first and second derivatives. Using the inverse kinematics

$$\boldsymbol{\omega}_{ib}^b = \mathbf{T}^{-1}(\boldsymbol{\Theta})\dot{\boldsymbol{\Theta}}, \tag{14}$$
$$\dot{\boldsymbol{\omega}}_{ib}^b = \dot{\mathbf{T}}^{-1}(\boldsymbol{\Theta})\dot{\boldsymbol{\Theta}} + \mathbf{T}^{-1}(\boldsymbol{\Theta})\ddot{\boldsymbol{\Theta}}, \tag{15}$$

we obtain the model

$$\mathbf{M}(\boldsymbol{\Theta})\ddot{\boldsymbol{\Theta}} = -\mathbf{C}(\boldsymbol{\Theta},\dot{\boldsymbol{\Theta}})\dot{\boldsymbol{\Theta}} - \mathbf{A}^*(\boldsymbol{\Theta})\boldsymbol{\tau}_a + \mathbf{T}^{-T}(\boldsymbol{\Theta})\boldsymbol{\tau}_d \tag{16a}$$
$$\mathbf{I}_s\dot{\boldsymbol{\omega}}_s = \boldsymbol{\tau}_a - \mathbf{I}_s\mathbf{A}\left[\dot{\mathbf{T}}^{-1}(\boldsymbol{\Theta})\dot{\boldsymbol{\Theta}} + \mathbf{T}^{-1}(\boldsymbol{\Theta})\ddot{\boldsymbol{\Theta}}\right], \tag{16b}$$

where

$$\mathbf{M}(\boldsymbol{\Theta}) = \mathbf{T}^{-T}(\boldsymbol{\Theta})\mathbf{J}\mathbf{T}^{-1}(\boldsymbol{\Theta}) \tag{17}$$
$$\mathbf{C}(\boldsymbol{\Theta},\dot{\boldsymbol{\Theta}}) = -\mathbf{T}^{-T}(\boldsymbol{\Theta})\mathbf{S}(\mathbf{J}\mathbf{T}^{-1}(\boldsymbol{\Theta})\dot{\boldsymbol{\Theta}} + \mathbf{A}\mathbf{I}_s\boldsymbol{\omega}_s)\mathbf{T}^{-1}(\boldsymbol{\Theta}) + \mathbf{T}^{-T}(\boldsymbol{\Theta})\mathbf{J}\dot{\mathbf{T}}^{-1}(\boldsymbol{\Theta}) \tag{18}$$
$$\mathbf{A}^*(\boldsymbol{\Theta}) = \mathbf{T}^{-T}(\boldsymbol{\Theta})\mathbf{A}. \tag{19}$$

It can also be shown the the matrices have the following properties

$$\mathbf{M} = \mathbf{M}^T > 0 \tag{20}$$
$$\mathbf{x}^T(\dot{\mathbf{M}} - 2\mathbf{C})\mathbf{x} \equiv 0, \forall\ \mathbf{x} \in \mathbb{R}^3 \tag{21}$$

2) Translational dynamics: The translational dynamics is derived for the case of formation flying in deep space, where the influence of other celestial objects is negligible. Under this assumption we model the translational dynamics as

$$m_b\mathbf{I}_{3\times 3}\ddot{\mathbf{p}}^i = \mathbf{R}_b^i\mathbf{f}_d^b + \mathbf{R}_b^i\mathbf{f}_c^b, \tag{22}$$

where m_b is the mass of the spacecraft, $\mathbf{p}^i$ is the inertial position of the center of gravity, $\mathbf{f}_d^b$ and $\mathbf{f}_c^b$ the disturbance and control forces respectively and $\mathbf{R}_b^i$ the rotation matrix between $\mathcal{F}_i$ and $\mathcal{F}_b$.

3) Complete 6 degrees of freedom model: A complete 6 DOF model may now be written as:

$$\mathbf{M}^*(\mathbf{x})\ddot{\mathbf{x}} = -\mathbf{C}^*(\mathbf{x},\dot{\mathbf{x}})\dot{\mathbf{x}} - \mathbf{B}_1(\mathbf{x})\mathbf{u} + \mathbf{B}_2(\mathbf{x})\mathbf{w}, \tag{23a}$$

where

$$\mathbf{x} \triangleq [\mathbf{p}^i, \boldsymbol{\Theta}]^T \tag{24}$$
$$\mathbf{u} \triangleq [\mathbf{f}_c, \boldsymbol{\tau}_a^b]^T \tag{25}$$
$$\mathbf{w} \triangleq [\mathbf{f}_d, \boldsymbol{\tau}_d^b]^T \tag{26}$$
$$\mathbf{M}^*(\mathbf{x}) = \begin{bmatrix} m_b\mathbf{I}_{3\times 3} & 0 \\ 0 & \mathbf{M}_{22}(\boldsymbol{\Theta}) \end{bmatrix} \tag{27}$$
$$\mathbf{C}^*(\mathbf{x},\dot{\mathbf{x}}) = \begin{bmatrix} 0 & 0 \\ 0 & \mathbf{C}(\boldsymbol{\Theta},\dot{\boldsymbol{\Theta}}) \end{bmatrix} \tag{28}$$
$$\mathbf{B}_1(\mathbf{x}) = \begin{bmatrix} \mathbf{R}_b^i & 0 \\ 0 & \mathbf{A}^*(\boldsymbol{\Theta}) \end{bmatrix} \tag{29}$$
$$\mathbf{B}_2(\mathbf{x}) = \begin{bmatrix} \mathbf{R}_b^i & 0 \\ 0 & \mathbf{T}^{-T}(\boldsymbol{\Theta}) \end{bmatrix} \tag{30}$$

Which retains the properties

$$\mathbf{M}^* = \mathbf{M}^{*T} > 0 \tag{31}$$
$$\mathbf{x}^T(\dot{\mathbf{M}}^* - 2\mathbf{C}^*)\mathbf{x} \equiv 0, \forall\ \mathbf{x} \in \mathbb{R}^3 \tag{32}$$

III. Control design

In this chapter we design a synchronization controller for attitude and position control of a spacecraft formation. The intuition behind the design is to develop a synchronization scheme such that the spacecraft are synchronized both with respect to a desired attitude and position trajectory and at the same time maintaining the formation by keeping the relative attitude and distance. This may be necessary during formation reconfiguration, to keep the spacecraft moving in a synchronized manner.

A. Synchronization error

Before we propose the controller we define the *mutual synchronization error* of the k'th spacecraft as

$$\mathbf{s}_k \triangleq \mathbf{x}_k - \mathbf{x}_{rk}, \tag{33}$$

where $\mathbf{x}_{rk}$ is defined by

$$\mathbf{x}_{rk} \triangleq \begin{bmatrix} \mathbf{K}_k \mathbf{p}^i_{dk} - \sum_{j=1, j\neq k}^n \mathbf{K}_{k,j}(\mathbf{p}^i_j - \mathbf{p}^i_k - \mathbf{p}^i_{dkj}) \\ \mathbf{\Theta}_d - \sum_{j=1, j\neq k}^n \mathbf{K}_{k,j}(\mathbf{\Theta}_j - \mathbf{\Theta}_k) \end{bmatrix}, \tag{34}$$

which may be viewed as a virtual reference trajectory, combining the goals of tracking a desired reference attitude and position trajectory and synchronizing with the other spacecraft in the formation.

Assuming negligible disturbances, the error dynamic can be written as

$$\mathbf{M}^*_k(\mathbf{x}_k)\ddot{\mathbf{s}}_k = -\mathbf{C}^*(\mathbf{x}_k, \dot{\mathbf{x}}_k)\dot{\mathbf{x}}_k - \mathbf{B}_1(\mathbf{x}_k)\mathbf{u}_k - \mathbf{M}^*_k(\mathbf{x}_k)\ddot{\mathbf{x}}_{rk}. \tag{35}$$

Proposition 1: The error dynamics (35), with control input

$$-\mathbf{B}_1(\mathbf{x}_k)\mathbf{u}_k \triangleq \mathbf{C}^*(\mathbf{x}_k, \dot{\mathbf{x}}_k)\dot{\mathbf{x}}_{rk} + \mathbf{M}^*_k(\mathbf{x}_k)\ddot{\mathbf{x}}_{rk} - \mathbf{K}_{p,k}\mathbf{s}_k - \mathbf{K}_{d,k}\dot{\mathbf{s}}_k, \forall\ k \in \{1, \dots, n\}, \tag{36}$$

where $\mathbf{K}_{p,k}$ and $\mathbf{K}_{d,k}$ are positive definite gain matrices, has a uniformly asymptotically stable (UAS) origin $(\mathbf{s}_k, \dot{\mathbf{s}}_k) = (\mathbf{0}, \mathbf{0}) \forall\ k \in \{1, \dots, n\}$, for all initial conditions $(\mathbf{s}_{k0}, \dot{\mathbf{s}}_{k0})$ in any ball about the origin not containing $\theta_k = \pm\frac{\pi}{2}$. Which implies UAS for the tracking error and the synchronization error.

Proof: By combining (35) and (36) the closed-loop error-dynamics can be written

$$\mathbf{M}^*_k(\mathbf{x}_k)\ddot{\mathbf{s}}_k + \mathbf{K}_{d,k}\dot{\mathbf{s}}_k + \mathbf{K}_{p,k}\mathbf{s}_k = \mathbf{C}^*(\mathbf{x}_k, \dot{\mathbf{x}}_k)\dot{\mathbf{s}}_k. \tag{37}$$

As the error-variable is actually a function of the system state and a time-varying reference signal, the system is non-autonomous. This implies that the often invoked Lasalle's invariance principle [21], is no longer applicable in the case of a semi-definite Lyapunov derivative. In this paper we remedy this by invoking Matrosov's theorem [22], as it was given in [23]. For ease of reference the theorem is summarized in appendix A. We now proceed to satisfy the four assumptions of the theorem.

Satisfying Assumption 1: Taking $V(\mathbf{s}, \dot{\mathbf{s}}, t)$ as the quadratic lyapunov function candidate

$$V = \sum_{k=1}^n \left[\tfrac{1}{2}\dot{\mathbf{s}}_k^T \mathbf{M}^*_k(\mathbf{x}_k)\dot{\mathbf{s}}_k + \tfrac{1}{2}\mathbf{s}_k^T \mathbf{K}_{p,k}\mathbf{s}_k\right], \tag{38}$$

which is clearly continuous and positive definite and decresent, we have satisfied the first assumption.

Satisfying Assumption 2: Taking the time derivative along solution trajectories and using (32), we obtain

$$\dot{V} = \sum_{k=1}^n \left[\dot{\mathbf{s}}_k^T \mathbf{M}^*_k(\mathbf{x}_k)\ddot{\mathbf{s}}_k + \dot{\mathbf{s}}_k^T \dot{\mathbf{M}}^*_k(\mathbf{x}_k)\dot{\mathbf{s}}_k + \dot{\mathbf{s}}_k^T \mathbf{K}_{p,k}\dot{\mathbf{s}}_k\right] \tag{39}$$

$$= \sum_{k=1}^n \dot{\mathbf{s}}_k^T \left[-\mathbf{K}_{d,k}\dot{\mathbf{s}}_k + \tfrac{1}{2}\dot{\mathbf{M}}^*_k(\mathbf{x}_k)\dot{\mathbf{s}}_k + \mathbf{C}^*(\mathbf{x}_k, \dot{\mathbf{x}}_k)\dot{\mathbf{s}}_k\right] \tag{40}$$

$$= \sum_{k=1}^n -\dot{\mathbf{s}}_k^T \mathbf{K}_{d,k}\dot{\mathbf{s}}_k = U(x) \leq 0. \tag{41}$$

Since the time derivative is negative semi-definite on any ball such that $\theta_k \neq \frac{\pi}{2} \forall k \in \{1, \dots, n\}$, $\dot{V}$ can be bounded by a non-positive and continuous function, which is independent of time. Hence the second assumption is satisfied.

Satisfying Assumption 3: We take $W(\mathbf{x}, t)$[1] as

$$W \triangleq \sum_{k=1}^n \dot{\mathbf{s}}_k \mathbf{K}_{p,k}\mathbf{s}_k. \tag{42}$$

As Assumption 2 implies a uniformly stable closed-loop system, the states $\mathbf{s}$ and $\dot{\mathbf{s}}$ are bounded, which in turn leads to the boundedness of $W(\mathbf{x}, t)$ satisfying the third assumption.

Satisfying Assumption 4: The final step is to show that when $\dot{V} = 0$, $\dot{W}$ is definitely non-zero. Taking the time-derivative of $\dot{W}$ along the solution trajectories of (37) we obtain

$$\dot{W} = \sum_{k=1}^n \left[\ddot{\mathbf{s}}_k^T \mathbf{K}_{p,k}\mathbf{s}_k + \dot{\mathbf{s}}_k \mathbf{K}_{p,k}\ddot{\mathbf{s}}_k\right], \tag{43}$$

which on the set $\mathbb{N}$, as defined in (61), can be written

$$\dot{W} = \sum_{k=1}^n -\mathbf{s}_k \mathbf{K}_{p,k}^T \mathbf{M}^{*T}_k(\mathbf{x}_k)\mathbf{K}_{p,k}\mathbf{s}_k \leq 0, \tag{44}$$

Since it is non-zero for any $\mathbf{s}_k \neq 0$ the last assumption is satisfied, and the system is *uniformly asymptotically stable* for any $(\mathbf{s}_{0k}, \dot{\mathbf{s}}_{k0})$ in any ball not containing $\theta_k = \pm\frac{\pi}{2}$.

Remark 2: The limitation in the area of attraction comes from an inherent singularity in the Euler angle representation of attitude. Possible methods of avoiding this problem do exist. One way, similar to what was done in [24], is to express the kinematics using a singularity free attitude representation like the unit quaternion, another possibility is to let the control system operate with two body frames and two sets of desired angles, such that the singularity can be avoided as in [25]. As the error would be the same, no discontinuities

[1] Notice that there is no requirement for $W(\mathbf{x}.t)$ to be positive definite

would appear in the control input, and an area of attraction covering the full state-space is achieved.

The next step is to show that UAS of the origin $(\mathbf{s}, \dot{\mathbf{s}}) = (\mathbf{0}, \mathbf{0})$ implies UAS of the tracking and synchronization errors. We first rewrite the synchronization error $\mathbf{s}_k$ in terms of the position and attitude errors as

$$\mathbf{s}_k = \begin{bmatrix} (\mathbf{K}_k - \sum_{j=1,j\neq k}^{n} \mathbf{K}_{k,j})\tilde{\mathbf{p}}_k^i - \sum_{j=1,j\neq k}^{n} \mathbf{K}_{kj}\tilde{\mathbf{p}}_j^i \\ \tilde{\mathbf{\Theta}}_{k,k} - \sum_{j=1,j\neq k}^{p} \mathbf{K}_{1,j}\tilde{\mathbf{\Theta}}_{k,j} \end{bmatrix} \tag{45}$$

where we have defined

$$\tilde{\mathbf{p}}_k^i \triangleq \mathbf{p}_{dk}^i - \mathbf{p}_k^i \tag{46}$$
$$\tilde{\mathbf{\Theta}}_{k,k} \triangleq \mathbf{\Theta}_d - \mathbf{\Theta}_k \tag{47}$$
$$\tilde{\mathbf{\Theta}}_{k,j} \triangleq \mathbf{\Theta}_j - \mathbf{\Theta}_k, \tag{48}$$

provided that the desired trajectory $\mathbf{p}_{dk}^i$, have been defined such that the relative distances are feasible. The synchronization errors can be written in terms of the tracking position errors and the attitude tracking and synchronization errors as (50) and (49). With proper selection of the gain matrices $\mathbf{K}_k$ and $\mathbf{K}_{k,j}$, such that the matrices $\mathbf{G}_1$ and $\mathbf{G}_2$, results in unique solutions to (50) and (49) given on the last page, we have that convergence of the synchronization errors $\mathbf{s}_k$ implies $\mathbf{\Theta}_k \to \mathbf{\Theta}_d$ and $\tilde{\mathbf{p}}_k \to 0$, $\forall k \in \{1, \ldots, n\}$.

Similarly, one can show the convergence $\dot{\mathbf{x}}_i \to \dot{\mathbf{x}}_d$. This concludes the proof. ■

IV. SIMULATIONS

We here present a simulation of the proposed synchronization scheme. We simulate a formation of 3 spacecraft, which have desired attitude and position trajectories, as well as desired relative distances.

TABLE I
MODEL PARAMETERS

Parameter	Value
Inertia matrix	diag$\{4, 4, 3\}$ $[kgm^2]$
Wheel inertia	$8 \cdot 10^{-3}$ $[kgm^2]$
Max wheel torque	0.2 $[Nm]$
Max wheel speed	400 $[rad/s]$
Max position thrust	10 $[N]$

$$\mathbf{p}_{1d}(t) = [t, 0, -t+5]^T [km] \tag{51}$$
$$\mathbf{p}_{1d}(t) = [t+1, 0, -t]^T [km] \tag{52}$$
$$\mathbf{p}_{1d}(t) = [t+1, 1, -t]^T [km] \tag{53}$$
$$\mathbf{\Theta}_d = 20^\circ \sin t \tag{54}$$
$$\tag{55}$$

Initial conditions are given by

$$\mathbf{x}_1 = [5\ km, 0\ km, 0\ km, 10^\circ, 0^\circ, 21^\circ]^T \tag{56}$$
$$\mathbf{x}_2 = [0\ km, 10\ km, 0\ km, -20^\circ, 10^\circ, 35^\circ]^T \tag{57}$$
$$\mathbf{x}_3 = [0\ km, -10\ km, 0\ km, 20^\circ, 20^\circ, -35^\circ]^T \tag{58}$$
$$\tag{59}$$

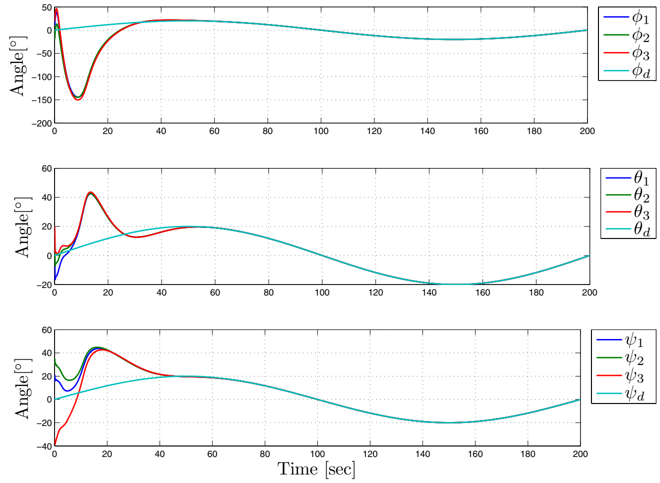

Fig. 3. The figure illustrates how the attitudes of the three spacecraft are first mutually synchronized, and then track a desired orientation.

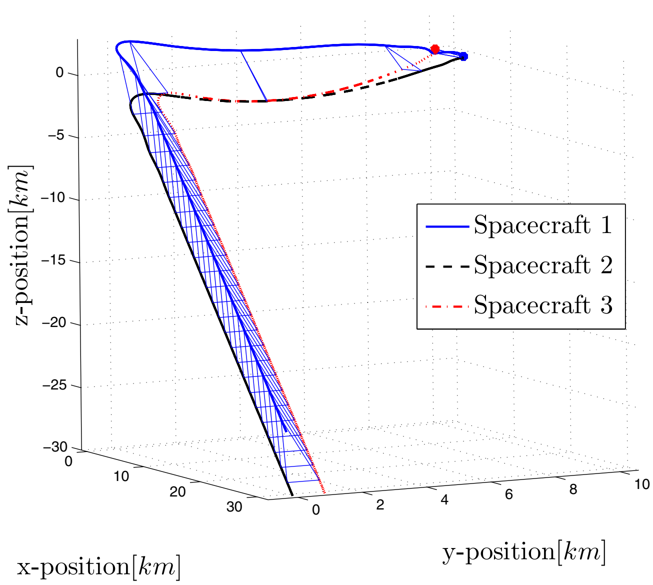

Fig. 4. Tracking and synchronization behaviour in position. All units are in km. The triangles indicate the relative position at different time-instants. The initial position is indicated by a *.

In this simulation the satellites are controlled to follow a straight line movement through space, while retaining a triangular formation. The common desired attitude is selected as a sinusoidal function of time.

Simulations show that the trajectories, for both position and attitude, are tracked and that the synchronization errors converge. This behaviour is decided by selecting the gains of the controller such that synchronization errors are more penalized than tracking error. By decreasing the gains on the synchronization error, we obtain a behaviour where the spacecraft move towards the desired trajectory individually rather than in a synchronized manner.

Remark 3: In the present design, collision avoidance is not implemented. One possibility is to implement a collision avoidance scheme on top of this low-level design.

$$\underbrace{\begin{bmatrix} (\mathbf{I}_{3\times3}+\sum_{j=1,j\neq1}^{n}\mathbf{K}_{1,j}) & -\mathbf{K}_{1,2} & \cdots & -\mathbf{K}_{1,n} \\ -\mathbf{K}_{2,1} & (\mathbf{I}_{3\times3}+\sum_{j=1,j\neq2}^{n}\mathbf{K}_{2,j}) & \cdots & -\mathbf{K}_{2,n} \\ \vdots & & \ddots & \\ -\mathbf{K}_{n,1} & -\mathbf{K}_{n,2} & \cdots & (\mathbf{I}_{3\times3}+\sum_{j=1,j\neq n}^{n}\mathbf{K}_{n,j}) \end{bmatrix}}_{\mathbf{G}_1} \begin{bmatrix} \mathbf{\Theta}_1 \\ \mathbf{\Theta}_2 \\ \vdots \\ \mathbf{\Theta}_n \end{bmatrix} = \begin{bmatrix} \mathbf{\Theta}_d \\ \mathbf{\Theta}_d \\ \vdots \\ \mathbf{\Theta}_d \end{bmatrix} \tag{49}$$

$$\underbrace{\begin{bmatrix} (\mathbf{K}_1-\sum_{j=1,j\neq1}^{n}\mathbf{K}_{1,j}) & -\mathbf{K}_{1,2} & \cdots & -\mathbf{K}_{1,n} \\ -\mathbf{K}_{2,1} & (\mathbf{K}_1-\sum_{j=1,j\neq2}^{n}\mathbf{K}_{2,j}) & \cdots & -\mathbf{K}_{2,n} \\ \vdots & & \ddots & \\ -\mathbf{K}_{n,1} & -\mathbf{K}_{n,2} & \cdots & (\mathbf{K}_n-\sum_{j=1,j\neq n}^{n}\mathbf{K}_{n,j}) \end{bmatrix}}_{\mathbf{G}_2} \begin{bmatrix} \tilde{\mathbf{p}}_1^i \\ \tilde{\mathbf{p}}_2^i \\ \vdots \\ \tilde{\mathbf{p}}_n^i \end{bmatrix} = \begin{bmatrix} 0 \\ 0 \\ \vdots \\ 0 \end{bmatrix} \tag{50}$$

V. CONCLUSION

In this paper we have given the design of 6 DOF mutual synchronization controller for a formation of spacecraft, similar to what has earlier been proposed for robotic manipulators. We have proved that the controller yields uniformly asymptotically stable error dynamics, such that all states converge to the desired states, in a synchronized manner. The proposition has been proved mathematically and its validity is demonstrated by numerical simulations.

APPENDIX

A. Matrosov's Theorem

Theorem 1 (Matrosov's theorem [23]): Given the system

$$\dot{x} = f(t, x) \tag{60}$$

Let two functions $V(x,t)$ and $W(x,t)$ be given which are continuous on the domain $\mathbb{D}$ and satisfy:

Assumption 1: $V(x,t)$ is positive definite and decresent.

Assumption 2: The derivative $\dot{V}$ can be bounded from above by a non-positive continuous t-independent function $U(x)$.

Assumption 3: The function $W(t,x)$ is bounded.

Assumption 4: The derivative $\dot{W}$ is definitely non-zero on the set

$$\mathbb{N} = \{x | U(x) = 0\}. \tag{61}$$

Then the equilibrium of (60) is uniformly asymptotically stable on $\mathbb{D}$.

REFERENCES

[1] A. Moreira, G. Krieger, I. Hajnsek, M. Werner, S. Riegger, and E. Settelmeyer, "Tandem-x: a terrasar-x add-on satellite for single-pass sar interferometry," in *Proceedings of the 2004 IEEE International Geoscience and Remot Sensing Symposium*, vol. 2, 2004, pp. 1000–1003.

[2] OHB System AG, "Sar-lupe: The innovative program for satellite-based radar reconnaissance," Brochure.

[3] ESA, "Xeus cdf report," ESA," Technical report, 2004.

[4] C. V. M. Fridlund, "Darwin - the infrared space interferometry mission," *ESA Bulletin*, vol. 100, pp. 20–25, 2000.

[5] H. Pan and V. Kapila, "Adaptive nonlinear control for spacecraft formation flying with coupled translational and attitude dynamics," in *Proceedings of the 40st IEEE Conference on Decision and Control*, 2001.

[6] W. Kang and H. Yeh, "Co-ordinated attitude control of multi-satellite systems," *International Journal of Robust and Nonlinear Control*, vol. 12, pp. 185–205, 2002.

[7] P. K. C. Wang, F. Y. Hadaegh, and K. Lau, "Synchronized formation rotation and attitude control of multiple free-flying spacecraft," *Journal of Guidance, Control and Dynamics*, pp. 28–35, 1999.

[8] H. Nijmeijer and A. Rodriguez-Angeles, *Synchronization of Mechanical Systems*, L. Chua, Ed. World Scientific, 2003.

[9] M. J. Mataric, "Minimizing complexity in controlling a mobile robot population," in *1992 IEEE Int. Conf. on Robotics and Automation Proceedings*, vol. 1, May 1992, pp. 830–835.

[10] T. Balch and R. C. Arkin, "Behavior-based formation control for multirobot teams," *IEEE Transactions on Robotics and Automation*, vol. 14, no. 6, December 1998.

[11] A. D. Mali, "On the behavior-based architectures of autonomous agency," *IEEE Transactions on Systems, Man and Cybernetics, Part C: Applications and Reviews*, vol. 32, no. 3, August 2002.

[12] J. R. T. Lawton, "A behavior-based approach to multiple spacecraft formation flying," Ph.D. dissertation, Bringham Young University, Dept. of El. and Comp. Engineering, November 2000.

[13] M. A. Lewis and K. Tan, "High precision formation control of mobile robots using virtual structures," *Autonomous Robots*, vol. 4, pp. 387–403, 1997.

[14] R. W. Beard, J. R. T. Lawtond, and F. Y. Hadaegh, "A coordination architecture for formation control," *IEEE Transactions on Control Systems Technology*, vol. 9, pp. 777–790, 2001.

[15] W. Ren and R. W. Beard, "Formation feedback control for multiple spacecraft via virtual structures," in *2004 IEEE Proceedings of Control Theory Application*, 2004.

[16] O. Egeland and J. T. Gravdahl, *Modeling and Simulation for Automatic Control*. Marine Cybernetics, 2001.

[17] P. C. Hughes, *Spacecraft attitude dynamics*. John Wiley & Sons, 1986.

[18] C. D. Hall, "Spinup dynamics of gyrostats," *Journal of Guidance, Control, and Dynamics*, vol. 18, no. 5, pp. 1177–1183, Sptember-October 1995.

[19] R. Wisniewski, "Lecture notes on modeling of a spacecraft," May 2000, [Available online:www.control.auc.dk/ raf/ModellingOfMech/Rep8sem.ps, Last accessed: 05.06.2005].

[20] T. R. Krogstad, J. T. Gravdahl, and R. Kristiansen, "Coordinated control of satellites," in *Proceedings of the 2005 International Astronautical Congress*, October 2005.

[21] H. Khalil, *Nonlinear Systems*, 3rd ed. Prentice Hall, 2002.

[22] V. M. Matrosov, "On the stability of motion," *Journal of Appl. Math. Mech.*, vol. 26, pp. 1337–1353, 1962.

[23] W. Hahn, *Stability of Motion*. Springer-Verlag, 1967.

[24] O.-E. Fjellstad and T. Fossen, "Position and attitude tracking of auv's: a quaternion feedback approach," *Oceanic Engineering, IEEE Journal of*, vol. 19, no. 4, pp. 512–518, 1994.

[25] P. Singla, D. Mortari, and J. L. Junkins, "How to avoid singularity when using euler angles?" in *Advances in the Astronautical Sciences*, vol. 119, no. II. Maui, HI, United States: Univelt Inc., San Diego, CA 92198, United States, 2005, pp. 1409–1426.